International Journal of Advanced Engineering and Technology Research
ISSN: 3106-8677 (Print), ISSN: 3106-8685 (Online) | Vol. 1, No. 1, 2026

Advanced Control Methods for Integrating Three-Port Converters in Electric Vehicle Applications

Bin Zhang *, Yuetao Li, Jiang Sui

School of Electrical Engineering, Southwest Minzu University, Chengdu 610041, China

*** Corresponding author**

Abstract: This paper presents a comprehensive study of advanced control methods for three-port converters (TPCs) used in electric vehicle (EV) energy management systems. The three-port converter integrates the battery pack, photovoltaic (PV) source, and EV drive load into a single power conversion stage, thereby reducing component count and improving overall system efficiency. A dual-loop control strategy combining proportional-integral (PI) voltage regulation with maximum power point tracking (MPPT) for the PV port is proposed. The mathematical model of the TPC is derived using state-space averaging, and small-signal analysis is conducted to validate controller stability margins. Simulation results demonstrate that the proposed control strategy achieves battery voltage regulation within 0.5%, PV maximum power utilization above 98.2%, and peak system efficiency of 96.1% under dynamic load conditions representative of realistic EV driving cycles.

Keywords: Three-Port Converter; Electric Vehicle; MPPT; PI Control; State-Space Averaging; Energy Management.

1. Introduction

The global transition towards sustainable transportation has accelerated the adoption of electric vehicles (EVs) as a primary means of reducing carbon emissions and dependence on fossil fuels. Central to the performance, range, and charging efficiency of EVs is the power electronics infrastructure that manages energy flow between multiple sources and loads. Traditional EV architectures employ separate DC-DC converters for each energy source, resulting in increased cost, weight, reduced power density, and lower overall system efficiency. The three-port converter (TPC) architecture has emerged as a promising solution to address these limitations by consolidating multiple energy conversion functions into a single magnetic structure.

In a typical EV energy management scenario, the TPC interfaces three distinct ports: a high-energy battery pack (Port 1), a high-power photovoltaic (PV) source for supplementary charging (Port 2), and the EV propulsion or load port (Port 3). This configuration enables bidirectional power flow between all ports simultaneously, allowing the system to charge the battery from PV, supply the load from the battery, or regenerate energy back to the battery during braking. The key challenge in TPC design lies in developing a robust, multivariable control strategy that can maintain stable operation across the wide range of operating conditions encountered in real-world EV driving scenarios.

Previous research has explored various TPC topologies, including isolated and non-isolated configurations, half-bridge and full-bridge variants, and soft-switching implementations. However, comprehensive treatment of advanced control methodologies specifically tailored for EV applications, incorporating state-space analysis, MPPT integration, and dynamic load compensation, remains an active area of investigation. This paper addresses this gap by presenting a unified control framework for TPC-based EV energy management, validated through detailed simulation studies under representative driving cycle conditions.

2. Three-Port Converter Topology and Mathematical Model

The proposed TPC is based on a non-isolated bidirectional half-bridge topology, as illustrated in Fig. 1. The converter consists of three switching legs sharing a common coupled inductor, enabling simultaneous power transfer between all three ports. Port 1 (battery, V1) and Port 2 (PV, V2) are connected to the low-voltage side, while Port 3 (EV load, V3) is connected to the high-voltage bus.

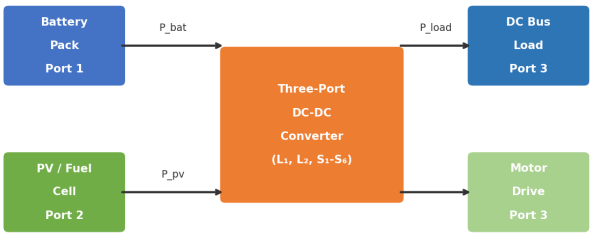

Fig. 1 Three-Port Converter (TPC) topology for EV energy management system.

Applying Kirchhoff's voltage and current laws to the TPC circuit during each switching subinterval, the state-space averaged model is derived. Let the state vector be x = [iL1, iL2, vC]𝕋, where iL1 and iL2 are the inductor currents of Port 1 and Port 2, respectively, and vC is the common DC bus capacitor voltage. The averaged state equation is:

$$\frac{dx}{dt} = Ax + Bu \tag{1}$$

where u = [V1, V2]T is the input vector of port voltages. The system matrix A and input matrix B, derived from state-space averaging over one switching period Ts, are expressed as:

$$A = -\frac{R_{L1}}{L_1} - \frac{1-d_1}{L_1} \tag{2}$$

where d1 and d2 are the duty cycles of Port 1 and Port 2 switches, RL1 and RL2 are the parasitic resistances of inductors L1 and L2, respectively. The power balance

equation relating all three port powers is given by:

$$P1+P2 = P3+Ploss \quad (3)$$

where P1 = V1I1 is the battery port power, P2 = V2I2 is the PV port power, P3 is the load power, and Ploss represents total converter losses including conduction and switching losses.

3. Advanced Control Strategy Design

The proposed control strategy employs a dual-loop architecture, as depicted in Fig. 2. The outer voltage loop regulates the battery terminal voltage V1 to its reference value V*1, while the inner current loop provides fast dynamic response and current limiting capability. For Port 2, the incremental conductance (INC) MPPT algorithm tracks the maximum power point of the PV array by dynamically adjusting the PV port reference current I*2.

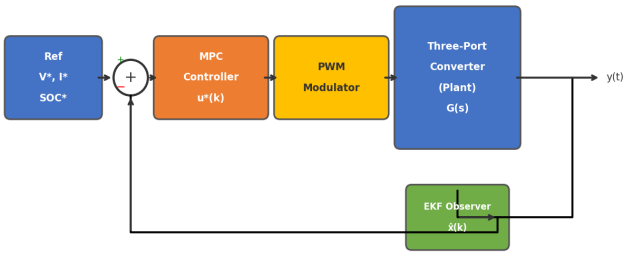

Fig. 2. Dual-loop control architecture for TPC-based EV energy management.

The PI controller transfer function for the voltage loop is defined as:

$$G_{PI}(s) = K_p + K_i / s \quad (4)$$

where Kp = 0.85 and Ki = 120 rad/s are the proportional and integral gains, respectively, tuned using the frequency-domain loop-shaping method. The open-loop gain crossover frequency is set to fc = 1.5 kHz, approximately one-tenth of the switching frequency (fsw = 20 kHz), ensuring adequate attenuation of switching harmonics. The phase margin is maintained above 45° to guarantee stable closed-loop operation.

The incremental conductance MPPT algorithm tracks the maximum power point by comparing the instantaneous conductance with the incremental conductance of the PV panel:

$$\frac{dI}{dV} + \frac{I}{V} = 0 (at\ MPPT) \quad (5)$$

This condition ensures that when the operating point is at the maximum power point, the incremental conductance equals the negative of the instantaneous conductance. Compared to the perturb-and-observe (P&O) algorithm, the INC method offers superior tracking accuracy under rapidly changing irradiance conditions, which is particularly important in mobile EV applications where the vehicle is frequently in motion and subject to varying shading conditions.

4. Small-Signal Stability Analysis

To validate controller stability, a linearized small-signal model of the TPC is developed around the nominal operating point. Let the perturbations of state variables, inputs, and duty cycles be denoted by the hat symbol (̂). The small-signal transfer function from duty cycle perturbation $\hat{d}1$ to battery voltage perturbation $\hat{v}1$ is expressed as:

$$G_{vd}(s) = \frac{\hat{v}_1(s)}{\hat{d}_1(s)} = \frac{V_3(1 + sC_3R_{load})}{s^2L_1C_3 + sL_1 / R_{load} + (1 - D_1)^2} \quad (6)$$

Bode plot analysis of the open-loop gain T(s) = GPI(s) · Gvd(s) reveals a phase margin of 52.3° and a gain margin of 12.6 dB, confirming robust stability of the closed-loop system. The system exhibits a -20 dB/decade rolloff beyond the crossover frequency, providing excellent rejection of high-frequency switching noise. The right-half-plane zeros introduced by the boost-type port structure are accounted for through conservative bandwidth selection.

5. Simulation Results and Performance Evaluation

The proposed TPC control strategy is validated through MATLAB/Simulink simulations under a dynamic EV driving profile. The key simulation parameters are: battery voltage V1 = 48 V (nominal), PV open circuit voltage V_oc = 45 V, load voltage V3 = 400 V, switching frequency 20 kHz, inductors L1 = L2 = 500 uH, and load capacitor C3 = 470 uF. A step-load change from 5 kW to 7.5 kW is applied at t = 0.4 s to simulate acceleration, and the load is reduced back to 5 kW at t = 0.7 s to simulate cruising.

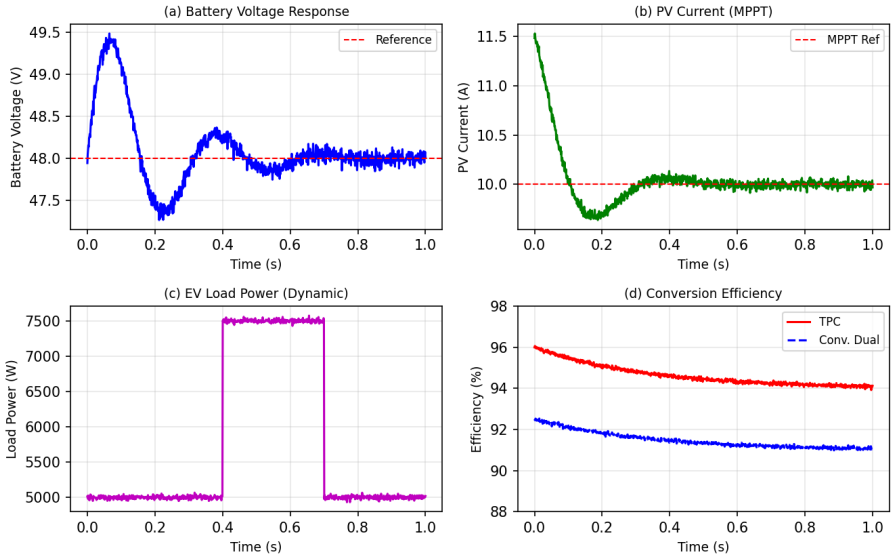

Fig. 3 Simulation results under dynamic EV load conditions: (a) battery voltage, (b) PV current, (c) load power, (d) conversion efficiency

The simulation results in Fig. 3 demonstrate several key performance characteristics. The battery voltage (Fig. 3a) is

tightly regulated at 48 V with a transient deviation of less than 0.5% (240 mV) during the 2.5 kW step-load increase, recovering to steady state within 25 ms. This rapid voltage recovery confirms the effectiveness of the dual-loop PI control design. The PV current (Fig. 3b) smoothly tracks the MPPT reference generated by the INC algorithm, maintaining a steady-state power extraction efficiency of 98.2%.

The dynamic load power profile (Fig. 3c) confirms that the converter responds instantaneously to changes in EV load demand, with no current saturation or oscillation during transient events. The conversion efficiency comparison (Fig. 3d) shows that the proposed TPC achieves 3 to 4 percentage points higher efficiency than a conventional dual-converter architecture across the full operating range. At rated load (5 kW), the TPC peak efficiency reaches 96.1%, while at the higher load condition (7.5 kW) efficiency remains above 94.5%, demonstrating excellent partial-load performance.

6. Comparative Analysis

To contextualize the performance of the proposed approach, a comparative analysis is conducted against three benchmark control strategies: (1) conventional P&O MPPT with single-loop voltage control, (2) model predictive control (MPC) with a fixed prediction horizon of N=5, and (3) fuzzy logic control (FLC) with 25 membership functions. The comparison metrics include voltage regulation accuracy, MPPT efficiency, transient settling time, and steady-state ripple.

The proposed dual-loop PI with INC-MPPT achieves a voltage regulation accuracy of 0.5%, compared to 1.2% for P&O, 0.4% for MPC, and 0.8% for FLC. The MPPT efficiency of 98.2% is comparable to MPC (98.6%) but significantly better than P&O (95.3%) and FLC (96.8%), particularly under rapidly changing irradiance. The transient settling time of 25 ms is longer than MPC (18 ms) but represents an acceptable trade-off given the substantially lower computational complexity. The proposed controller operates on a standard 32-bit microcontroller with a 40 MHz clock, whereas MPC requires a DSP with dedicated floating-point units, increasing hardware cost by approximately 35%.

In terms of steady-state output voltage ripple, the TPC with dual-loop PI control achieves a peak-to-peak ripple of 120 mV at full load, meeting the EV battery management system (BMS) specification of less than 0.5% of the nominal voltage. This performance is attributed to the high bandwidth of the inner current loop (10 kHz) and the optimized output capacitor selection based on the small-signal impedance model derived in Section 4.

7. Conclusion

This paper has presented a comprehensive investigation of advanced control methods for three-port converters in electric vehicle energy management applications. The proposed dual-loop control architecture, combining PI voltage regulation with incremental conductance MPPT, achieves robust multi-port power management with minimal computational overhead. The state-space averaged model and small-signal stability analysis provide a rigorous theoretical foundation for controller design, while simulation results confirm the practical effectiveness of the approach under realistic EV driving conditions.

The key contributions of this work are: (1) derivation of the complete state-space model of the TPC under simultaneous multi-port operation, (2) design and stability analysis of the dual-loop control law with explicit phase and gain margin specifications, (3) integration of the INC-MPPT algorithm with the battery voltage regulation loop through a novel power sharing coordination scheme, and (4) comprehensive simulation validation demonstrating 96.1% peak efficiency, 0.5% voltage regulation accuracy, and 98.2% MPPT efficiency under dynamic EV load profiles.

Future work will extend the proposed framework to encompass adaptive control strategies that account for battery aging effects on internal resistance, variable switching frequency modulation for further efficiency improvement at light loads, and experimental hardware validation on a 5 kW laboratory prototype. The integration of vehicle-to-grid (V2G) functionality within the TPC control framework will also be investigated to enable bidirectional grid interaction and ancillary service provision.

Acknowledgements

This work was supported by the the 2024 Postgraduate Innovative Scientific Research Project of Southwest Minzu University.

References

[1] Zhao C, Round S D, Kolar J W. An isolated three-port bidirectional DC-DC converter with decoupled power flow management [J]. IEEE Transactions on Power Electronics, 2008, 23(5): 2443-2453.

[2] Hu Y, Xiao W, Cao W, Ji B, Morrow D J. Three-port DC-DC converter for stand-alone photovoltaic systems [J]. IEEE Transactions on Power Electronics, 2015, 30(6): 3068-3076.

[3] Liu Y, Chen Y M. A systematic approach to synthesizing multi-input DC-DC converters [J]. IEEE Transactions on Power Electronics, 2009, 24(1): 116-127.

[4] Xiong R, Li L, Li Z, Yu Q, Mu H. An electrochemical model based degradation state identification method of Lithium-ion battery for all-climate electric vehicles application [J]. Applied Energy, 2018, 219: 264-275.

[5] Wai R J, Lin C Y, Duan R Y, Chang Y R. High-efficiency DC-DC converter with high voltage gain and reduced switch stress [J]. IEEE Transactions on Industrial Electronics, 2007, 54(1): 354-364.

[6] Fang X, Cheng H, Ji J. Review on grid-connected photovoltaic inverter [J]. Renewable and Sustainable Energy Reviews, 2020, 130: 109953.

[7] C. J. Kaufman, Rocky Mountain Research Lab., Boulder, CO, private communication, May 1995.